Geophysical Research Letters

RESEARCH LETTER
10.1029/2018GL078679

Key Points:
- Satellites detect only 25% of open biomass fire area and poorly resolve interannual fire variability in Florida and areas with similar fire regimes
- Fire area may decrease during drought in regions with extensive prescribed fire, like Florida, despite increases in wildfire
- Prescribed fires in the southeastern United States have a large day-of-week cycle that is missing from air pollutant emission inventories

Supporting Information:
- Supporting Information S1

Correspondence to:
H. K. Nowell,
hak07@my.fsu.edu

Citation:
Nowell, H. K., Holmes, C. D., Robertson, K., Teske, C., & Hiers, J. K. (2018). A new picture of fire extent, variability, and drought interaction in prescribed fire landscapes: Insights from Florida government records. *Geophysical Research Letters*, *45*. https://doi.org/10.1029/2018GL078679

Received 8 MAY 2018
Accepted 17 JUL 2018
Accepted article online 25 JUL 2018

A New Picture of Fire Extent, Variability, and Drought Interaction in Prescribed Fire Landscapes: Insights From Florida Government Records

H. K. Nowell[1], C. D. Holmes[1], K. Robertson[2], C. Teske[2], and J. K. Hiers[2]

[1]Department of Earth, Ocean, and Atmospheric Science, Florida State University, Tallahassee, FL, Florida, [2]Tall Timbers Research Station and Land Conservancy, Tallahassee, FL, Florida

Abstract Florida, United States, government records provide a new resource for studying fire in landscapes managed with prescribed fire. In Florida, most fire area (92%) is prescribed. Current satellite fire products, which underpin most air pollution emission inventories, detect only 25% of burned area, which alters airborne emissions and environmental impacts. Moreover, these satellite products can misdiagnose spatiotemporal variability of fires. Overall fire area in Florida decreases during drought conditions as prescribed fires are avoided, but satellite data do not reflect this pattern. This pattern is consistent with prescribed fire successfully reducing overall fire risk and damages. Human management of prescribed fires and fuels can, therefore, break the conventional link between drought and wildfire and play an important role in mitigating rising fire risk in a changing climate. These results likely apply in other regions of the world with similar fire regimes.

Plain Language Summary Wildfires and prescribed (i.e., controlled) fires are major sources of air pollution, greenhouse gases, and aerosols. Accurately estimating emissions from fires is critical to understanding their impacts on the environment and for designing sound fire management policies. We show that for Florida, United States, current satellites—the primary tools for identifying the extent, location, and time of these fires—dramatically underestimate the amount of fire, poorly identify its variation in space and time and can mischaracterize its relationship to drought. Using government records of fires, where available, can overcome some satellite shortcomings and provide a more accurate picture of fire extent and variability. In Florida, these records show that land area consumed by fire decreases during drought conditions due to less prescribed burning, but this pattern is not detected by satellites. Similar results may be expected in other parts of the world with similar fire characteristics, including agricultural and savanna regions of South America, Africa, Europe, and Asia. Using prescribed fire can help land managers adapt to climate-driven changes in wildfire activity.

1. Introduction

Vegetation fires are major sources of air pollutants and climate-forcing agents that degrade air quality and perturb regional and global climate (Al-Saadi et al., 2008; Bond et al., 2013; Brey et al., 2018; Dwyer et al., 2000; Kaulfus et al., 2017; Randerson et al., 2012; Schroeder et al., 2016; Schultz et al., 2008; Soja et al., 2006, 2011; Tosca et al., 2010; van der Werf et al., 2010). Satellite observations are critical for quantifying fires and these impacts over most of the globe because ground-based fire reporting is uncommon and may be incomplete (Giglio et al., 2009; Hawbaker et al., 2017b; Soja et al., 2006; van der Werf et al., 2017; Wiedinmyer et al., 2010). Current satellite-based fire data sets have been evaluated extensively in landscapes dominated by large wildfires, where high-quality ground-based data are available, and generally perform well (Giglio et al., 2009; Randerson et al., 2012; Soja et al., 2006). However, small, prescribed fires contribute a large fraction of global fire area (Randerson et al., 2012). There are limited data to assess satellite performance in detecting these small fires (Amiro et al., 2001; Eidenshink et al., 2007; Kasischke et al., 2002; Laris, 2005; Marques et al., 2011; McCarty et al., 2009; NIFC, 2012; Parisien et al., 2006), but available information suggests that many of them are undetected (Al-Saadi et al., 2008; Hu et al., 2016; Larkin et al., 2014; Soja et al., 2009).

The southeastern United States burns more land area than the rest of the contiguous United States combined, and Florida accounts for over 10% of all fire area in the United States (EPA, 2016; Melvin, 2015;

Randerson et al., 2017). Most of these fires are prescribed fires for agriculture, forestry, conservation, and wildfire mitigation, and most of them are small, under 20 ha (0.02 km^2) in size. These small, prescribed fires are difficult to detect from space due to their short duration (hours or less), low intensity, and small size relative to the resolution of many satellite instruments (Giglio et al., 2003; Hawbaker et al., 2008; Hu et al., 2016; McCarty et al., 2009; Yokelson et al., 2011; Zhu et al., 2017). Unlike many other regions, however, records of these prescribed fires are available from Florida and some other U.S. state governments. The southeastern United States, therefore, provides a valuable test case for evaluating the performance of satellite-based fire products in detecting small and prescribed fires, which are widespread globally. Florida's fires also occur on land cover types that host a large fraction of global fire activity (cropland, rangeland, savanna, grassland, shrubland, and temperate forest; van der Werf et al., 2017).

Satellite sensors can detect fires from thermal infrared signatures of active fires, changes in surface reflectance, which linger after the fire ceases, or both. All of these approaches face challenges in the southeastern United States. Active fires may be undetected if they burn under clouds, under tree canopies (typical of silvicultural fires), or when no satellite is overhead at the time of the fire (Cardoso et al., 2005; Giglio & Schroeder, 2007; Hawbaker et al., 2008; Prins et al., 1998). After a fire, vegetation can regrow quickly in the humid climate of the southeastern United States and obscure reflectance signatures of burned area before the next cloud-free satellite overpass (Picotte & Robertson, 2011). In Georgia, one common satellite product detected only 12% of fires and 60% of their total area (Hu et al., 2016, using Hazard Mapping System). For cropland fires, which are important in the southeastern United States and elsewhere, another product detected only 13% of burned area in Asia (Zhu et al., 2017, using Moderate Resolution Imaging Spectroradiometer, MODIS). Both of those studies, however, were limited to one year, so broader evaluations are needed.

Our work presents insights from a comprehensive data set of open biomass fires, meaning prescribed fires and wildfires, based on government reporting data in Florida. The data set provides a new tool for detecting patterns and trends of open fires and for evaluating remotely sensed products. These results can be applied to other regions of the world that have similar fire characteristics but lack comprehensive ground records. Government records avoid the fire detection challenges of remote sensing but require a critical assessment of their accuracy, which we do through comparisons to high-quality spatial fire records maintained by several land management organizations in Florida (sections 2 and 3). We show that the government data represent the magnitude and patterns of fires with similar or better accuracy to the common satellite-based methods in this region. We then examine the spatiotemporal patterns of prescribed fires and wildfires, including their relationship to climate variables (section 4), assess the ability of several common satellite-based fire products to detect these patterns, and discuss the other regions across the world that would likely have similar results to Florida (section 5).

2. Fire Data Sources and Methods

Prescribed fires in Florida are regulated by the Florida Forest Service (FFS), a state agency. Among the regulations, fire managers in Florida are required to request and obtain an open burn authorization (OBA) from FFS before starting a prescribed fire (Florida Statute, 2004). FFS generally approves OBA requests when weather conditions allow safe burning, provide good smoke dispersion, minimize smoke impacts on sensitive areas (roads, residential areas, hospitals, etc.), and when emergency response resources are available (Peterson et al., 2018). Approved OBAs are saved in a database that provides a comprehensive historical record of prescribed fire in Florida.

FFS provided us with anonymized OBA records of every authorized fire during 2004–2015. Each OBA includes a point location (latitude and longitude), date, burn area requested, and purpose (silviculture, agriculture, or land clearing for development). The FFS silviculture category includes commercial forestry and wildland management fires in forest, savanna, and shrubland. Pile burns are also recorded but not analyzed here. The accuracy of the FFS database requires evaluation because there are several potential sources of error. For example, location inaccuracies can occur when fire managers provide FFS with imprecise coordinates, a street address, or township and range within the Public Land Survey System, which FFS then converts to latitude and longitude. Area inaccuracies can occur when managers cancel a prescribed fire after an OBA is issued, or if part of the requested area contains ponds or other unburnable terrain. Since OBA requests are often approved in Florida, there is little incentive for land managers

to deliberately underestimate burn area or to avoid requesting permits. Therefore, our expectation is that OBAs may oveestimate burned area.

We evaluate the accuracy of the FFS database against comprehensive, high-quality prescribed fire records from four large sites in Florida (Table S1 and Figure S1 in the supporting information): Tall Timbers Research Station (TTRS, a private entity), Avon Park Air Force Range, Eglin Air Force Base, and Tyndall Air Force Base. These four evaluation sites comprise 4% of Florida's land area and 5% of the FFS-authorized fire area during the study period. Each landowner's fire records include the dates, areas, and fire perimeter polygons of all prescribed fires that occurred during 2004–2015. The perimeters are either mapped by GPS after a fire or are predetermined tracts that were previously mapped by GPS and are routinely burned as a block. At TTRS, the burned area calculated from predetermined tracts differed from a subset of postfire measurements using GPS by 5% or less, so both are sufficiently accurate for our purposes. We match each fire recorded by a land manager with the nearest FFS OBA issued for the same day (Figure S2 and Text S1). The difference in area and location between the OBA and known fire is considered error in the OBA database.

Wildfire information for Florida was obtained from the Fire Program Analysis Fire Occurrence Database (FPA FOD; Short, 2014, 2017). The FPA FOD combines wildfire reports from federal, state, tribal, and local governments, making it the most comprehensive database available for Florida and the United States. Nevertheless, it may omit some small wildfires, including fires on private land that were managed entirely by private fire crews.

We compare the Florida OBA and FPA FOD wildfire records to several widely used satellite data sets: the National Oceanic and Atmospheric Administration Hazard Mapping System (HMS; National Oceanic and Atmospheric Administration, 2017; Ruminski et al., 2006), Landsat Burned Area Essential Climate Variable (BAECV version 1.1; Hawbaker et al., 2017a, 2017b), and the Global Fire Emissions Database (GFED version 4.1s; Randerson et al., 2017). HMS uses thermal detections of active fires from multiple satellites (1–4 km resolution), while BAECV uses Landsat-series sensors (30-m resolution) to detect burn scars from changes in surface reflectance. GFED combines both of these approaches using MODIS data (0.5-km sensor reported at 0.25°; Giglio et al., 2013; Randerson et al., 2012, 2017), classifying fires as small if they are detected by thermal anomalies but not detected by the MODIS burned area product (MCD64A1; van der Werf et al., 2017). BAECV and GFED both provide fire area, but HMS does not. For HMS, we assume an average size of 19 ha per fire detection, which is the average size of HMS-detected fires in Georgia (Text S2; Hu et al., 2016). In addition, we examine an agriculture fire product used in the 2014 National Emission Inventory (NEI; Pouliot et al., 2017) and the Monitoring Trends in Burn Severity product (MTBS; USDA-FS & USGS, 2018), which includes only large fires (>202 ha in the Eastern United States; Eidenshink et al., 2007). We also relate the fire variability to the Palmer Drought Severity Index (PDSI; Heddinghaus & Sabol, 1991; Palmer, 1965), normalized against data from 1931 to 1990, and the Keetch-Byram Drought Index (KBDI; Keetch & Byram, 1968). Both indices are calculated from precipitation and air temperature, but KBDI is sensitive to subseasonal moisture changes that affect fine fuels, while PDSI tracks prolonged moisture imbalance that persists for months to years and affects deep soil moisture and deep-rooted plants.

3. Evaluation of Florida Open Burn Authorizations

The four study sites conducted 4,300 prescribed fires during 2004–2015. All but 198 can be matched with an FFS OBA, meaning that the state database contains 95.4% of known prescribed fires. The median difference between the area of a fire and its OBA ranges from −0.4% to −13% (0.1 to 11 ha, range across our four study sites), so fires are typically a little smaller than requested. However, the range of error among individual fires is −37% to +23% of the OBA area (±20%–25% median absolute deviation). Few fires (20%–28%) differ from their OBA area by more than a factor of two (Figure S3); most of those are smaller than authorized. Other measures of FFS OBA accuracy are summarized in Table S1 and Figure S3.

The metrics above reflect the accuracy of the OBAs for a single fire on a single day. Accuracy of time-averaged burn area is a better measure of the ability of OBAs to represent the overall extent and distribution of fires in Florida. Accumulated over the study years, the actual fire area at the four study sites ranged from 14% less than to 18% more than the OBA total (Table S1). Aggregated over all test sites and years, the OBA database has a cumulative area error of 9% (i.e., 504,000 ha in OBAs versus 555,000 ha mapped as burned). Thus, the OBA fire area has a typical error of 20%–40% for any given location and day, but the errors are under 20% at a

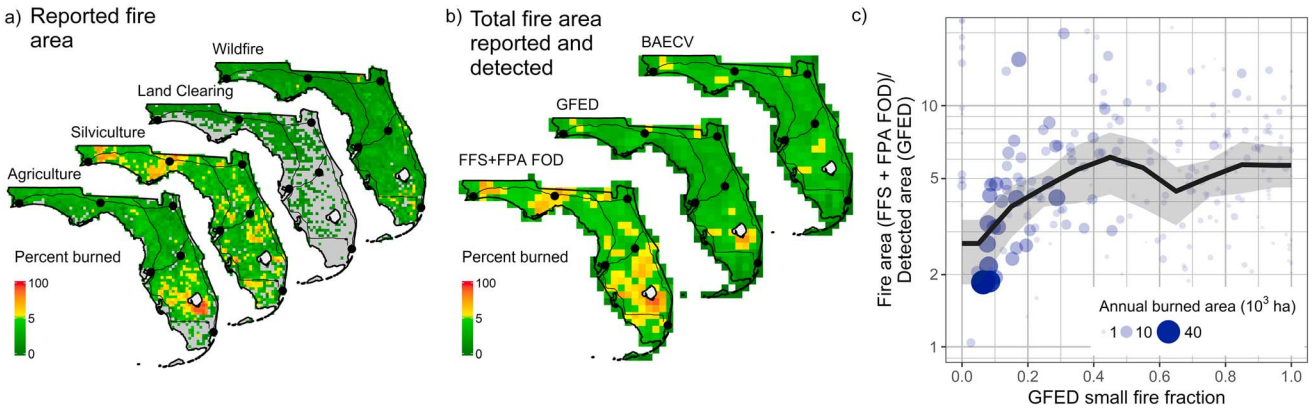

Figure 1. Mean annual burned area in Florida during 2004–2015 for (a) four fire types reported by FFS OBA (this work) and FPA FOD (Short, 2017), (b) total fires compared to satellite products (GFED version 4.1s and Landsat BAECV version 1.1; van der Werf et al., 2017; Hawbaker et al., 2017a), and (c) the ratio of reported to detected fire area. Panel a uses 0.1° resolution; panel b uses the 0.25° GFED grid to aid comparisons. Note the change in color scale at 5%. Lines are major highways and dots represent major cities. Panel c shows the ratios for each grid cell in Florida. The black line and shading show the mean ratio, weighted by fire area, and its 95% confidence interval (Text S5). FFS OBA = Florida Forest Service open burn authorization; FPA PPOD = Fire Program Analysis Fire Occurrence Database; GFED = Global Fire Emissions Database; BAECV = Burned Area Essential Climate Variable.

single site when averaged over the study period, and less, around 10%, when averaged over large regions of the state. For comparison, common satellite products may miss 40%–90% of fire area in the southeastern United States or in other agricultural regions (Hu et al., 2016; Zhu et al., 2017).

OBA location errors were 0.7–0.8 km (median, Table S1) and fewer than 20% of OBAs were located more than 2 km away from the actual fire (Figure S3). Although modest, these displacement errors mean that most OBA point locations are outside the actual fire perimeter (50%–98% of fires, Table S1), particularly for small fires and when a single OBA is requested for multiple fires, which is common at TTRS. As a result, OBAs can represent the general distribution of fires within Florida, but not the exact location of individual fires.

Table 1
Open Fire Characteristics for the Entire State of Florida During 2004–2015 Compared With Satellite-Based Fire Products[a]

	Number (year^{-1})	Area (10^3 ha/year)
Prescribed (FFS)		
Agriculture	15,180 ± 1,380	354 ± 31
Silviculture	6,480 ± 710	553 ± 67
Land clearing	240 ± 50	3 ± 1
Total prescribed	21,900 ± 1,800	909 ± 88
Wildfire (FPA FOD)	3,270 ± 1,100	78 ± 56
Total	25,160 ± 1,400	987 ± 73
Satellite products		
GFED[b]	—	268 ± 53
BAECV[c]	—	235 ± 91
MTBS[d]	200 ± 160	189 ± 121
HMS[e]	14,440 ± 3,020	274 ± 57
NEI/HMS agriculture[f]	—	92

Note. FFS = Florida Forest Service; FPA PPOD = Fire Program Analysis Fire Occurrence Database; GFED = Global Fire Emissions Database; BAECV = Burned Area Essential Climate Variable; MTBS = Monitoring Trends in Burn Severity; HMS = Hazard Mapping System; NEI = National Emission Inventory.
[a]Values are mean ± standard deviation across years [b]Version 4.1s (van der Werf et al., 2017) [c]Version 1.1 (Hawbaker et al., 2017a) [d]USDA-FS and USGS (2018) [e]NOAA (2017). Area assumes an average size of 19 ha per detection. See Text S2 [f]Data for 2014 only (Pouliot et al., 2017)

4. Current Status of Prescribed Fires, Wildfires, and Their Drought Interactions

Having established the accuracy of FFS prescribed fire data, we combine it with FPA FOD wildfire data to examine the patterns and variability of all open fires in Florida. Prescribed fires vastly exceed wildfires in Florida by area and number, as seen in Figure 1 and Table 1. Over the period 2004–2015, fires burned 9.9 ± 0.7 × 10^5 ha/year in Florida (multiyear mean ± standard deviation), which is 7% of the state's land area each year. Wildfires burned only 8% of this fire area (0.8 ± 0.6 × 10^5 ha/year). Of the prescribed fire types, silviculture fires consumed the most area (5.5 ± 6.7 × 10^5 ha/year), burning 50% more than agricultural fires. However, agricultural fires were much more numerous (15,000 year^{-1} versus 6,000 year^{-1}), reflecting their smaller average size (Figure S4). Figure 1a shows that most silviculture and land-clearing fires occur in northwest Florida, while agricultural fires dominate south Florida especially around Lake Okeechobee, where sugarcane agriculture is concentrated. Wildfires occur all across the state, but their area is concentrated in south Florida.

Prescribed fires in Florida are much more extensive on weekdays (Monday–Friday) than weekends (Figures 2a and S5). On Tuesday–Thursday, fires burn 3,400 ha/day compared to 1,000–1,500 ha/day on Saturday and Sunday. Monday and Friday are intermediate.

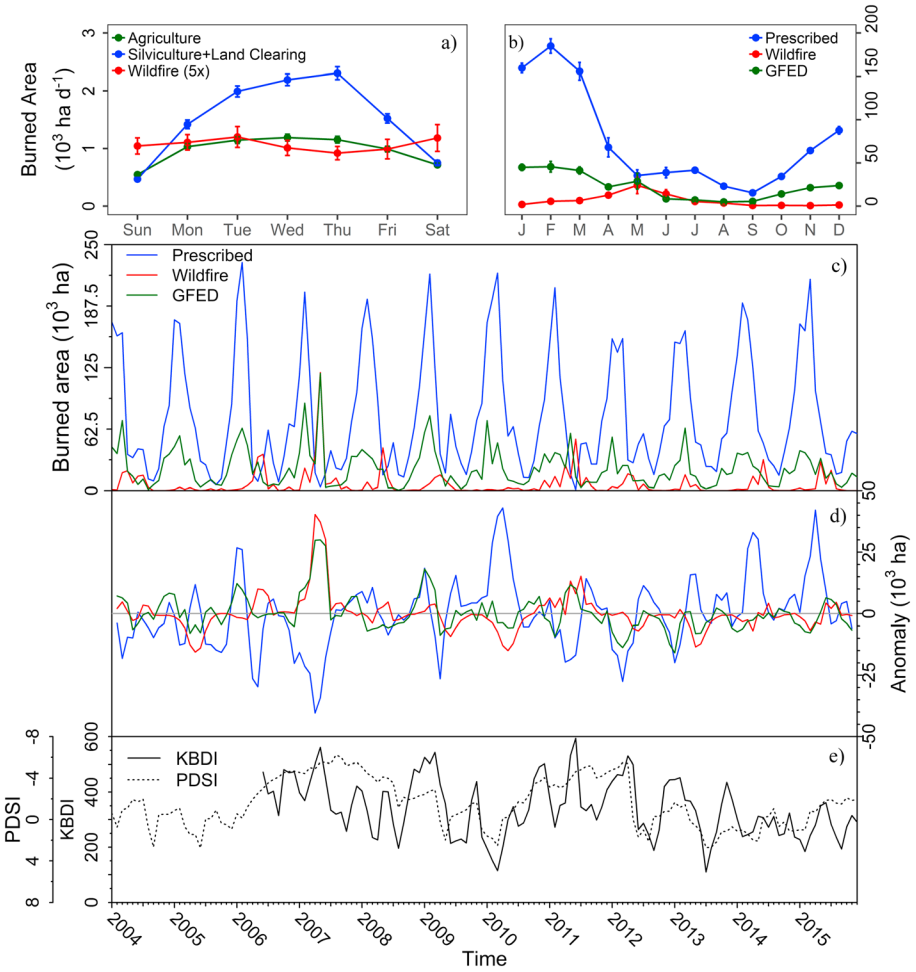

Figure 2. Fire area in Florida (a) by day of week, (b) by seasonal cycle, (c) monthly over the study period, and (d) monthly anomalies, with (e) drought indices for comparison. Prescribed fire data from Florida Forest Service (this work), wildfire data from Fire Program Analysis Fire Occurrence Database (Short, 2017), and Global Fire Emissions Database (GFED) from version 4.1s (van der Werf et al., 2017). Vertical lines in panels a and b show standard errors of the mean, which is smaller than some plot symbols. Anomalies in panel d are calculated with respect to the median annual cycle, shown in panel b, and smoothed with a 3-month running mean. Drought indices are the Palmer drought severity index (PDSI) and Keetch-Byram drought index (KBDI), both averaged over Florida. Dry conditions are associated with negative PDSI and large positive KBDI. The PDSI axis is reversed so that up indicates drought for both KBDI and PDSI.

Although this weekly cycle might be expected from labor customs, the NEI of air pollutants does not account for it (Text S3 and Figure S5; EPA, 2015a, 2015b, 2016, 2017, 2018) nor do past regional studies mention it (Larkin et al., 2014; Park et al., 2007; Schichtel et al., 2017; Schweizer et al., 2017; Zeng et al., 2008). Moreover, the day-of-week effect seen here for prescribed fires in Florida is much stronger than what NEI specifies for emissions in any state (see Text S3 and Figure S5; EPA, 2015a, 2015b, 2016, 2017, 2018). Surrounding states likely have similar weekly cycles of fire emissions and including them could improve future emission inventories. In contrast, wildfires in Florida show no weekly cycle (Figure 2a).

Prescribed fires and wildfires have different seasonal cycles (Figure 2b) and longer-term variability (Figures 2c and 2d). Prescribed fires are usually most active in December through April, because managers and government agencies prefer burning during cool and wet conditions for fire control and safety. Florida's wildfires peak in late spring, which is warmer and drier. On multiyear time scales, wildfire and prescribed fire area anomalies—the residual variability after removing the median seasonal cycle—are anticorrelated ($R = -0.53$, $R^2 = 0.28$, $p < 0.001$), meaning that years with extensive wildfires have below-normal prescribed fire area and vice versa.

As seen in Figures 2c–2e, wildfire area increases during dry conditions ($R^2 = 0.28$, 0.22 for area anomalies versus PDSI and KBDI drought indices, respectively, $p < 0.001$). In particular, a prolonged drought identified by PDSI from 2006 to 2008 produced three of the four highest wildfire area anomalies in the record. This pattern of wildfires increasing during drought is common around the world (Balch et al., 2015; Charlès, 2017; Prichard et al., 2017; Westerling et al., 2006). The link between drought and prescribed fire, which has been studied much less, follows a different pattern that is not detected by satellite burned area data sets (section 5). In Florida, prescribed fires are less extensive during dry conditions. This decline during drought is driven by a combination of land managers choosing not to burn as well as FFS denying authorizations. Prescribed fire area is more strongly anticorrelated with short-term drought (KBDI $R^2 = 0.28$, $p < 0.001$) than with long-term drought (PDSI $R^2 = 0.14$, $p < 0.001$), likely because KBDI, not PDSI, is used by FFS and others to predict fire risk. This means that prescribed fires can be and are conducted during long-term drought, as long as sufficient precipitation falls to occasionally moisten shallow soil and fine fuels.

Prescribed fire area dwarfs wildfire area in Florida by a factor of 12 during our study period (Table 1). As a result, during drought conditions the total fire area decreases because the prescribed fire area decreases. Figure 2d shows that the largest reductions (i.e., negative anomalies) in prescribed fires occurred during the 2006 to 2008 drought and are as large, or larger, than the simultaneous wildfire increase. Conversely, in wet years, like 2010 and 2013–2015, wildfires burned slightly less area than normal while prescribed fire area increased much more. These patterns repeat throughout the data set. Overall, anomalies in total fire area in Florida are uncorrelated with long-term drought (PDSI: $R = 0.12$, $R^2 = 0.01$, $p = 0.17$) and anticorrelated with short-term drought (KBDI: $R = -0.34$, $R^2 = 0.12$, $p < 0.001$). Using the standardized precipitation index shows the same relationships with drought on multiple time scales. A more detailed discussion can be found in Text S4 (Hall & Brown, 2003; McKee et al., 1993; Vicente-Serrano et al., 2010). The lack of overall fire increase during drought suggests that prescribed fire policy is succeeding on a large scale to reduce fire risks to people and property in Florida.

Numerous case studies of individual wildfires show that prior prescribed fires can reduce the occurrence, severity, and area of wildfire (Fernandes & Botelho, 2003 and references therein), but there is much less evidence of whether current levels of prescribed fire are achieving their risk reduction goals on larger state or regional scales (Addington et al., 2015; Prestemon et al., 2010). Wildfire risk assessments should recognize the dominance of prescribed fire in the southeastern United States and account for the complex relationships, shown here, between drought and different fire types. However, recent assessments have not accounted for these features (Balch et al., 2017; Prestemon et al., 2016; Stephens et al., 2013). As a result, their prediction of large increases in wildfire activity in the southeastern United States in future climate scenarios may be overstated (Liu et al., 2013; Prestemon et al., 2016).

5. Evaluation of Satellite-Based Fire Area Products

The Florida fire data provide a new tool for evaluating the accuracy of satellite-based fire products over a large region with multiple fire types that are common worldwide. Since the satellite sensors have resolutions of 30 m to 4 km while OBAs are typically 0.5–1 km away from actual fires (section 3), the OBAs are not expected to exactly overlap space-borne detections of the same individual fires. As a result, we conduct comparisons at coarser spatial resolution (Figure 1, Table 1).

Over 2004–2015, GFED detected fires covering $2.7 \pm 0.5 \times 10^5$ ha/year in Florida, BAECV detected $2.4 \pm 0.9 \times 10^5$ ha/year, and HMS detected $2.7 \pm 0.6 \times 10^5$ ha/year. All of these are far less than the actual total fire area of $9.9 \pm 0.7 \times 10^5$ ha/year recorded by the FFS OBA and the FPA FOD (Table 1). Although there is some uncertainty in the HMS burned area, the total is certainly less than actual fire area (Text S2). Large biases also appear in specialized fire databases that rely on satellite data. For example, MTBS reported only $1.9 \pm 1.2 \times 10^5$ ha/year across Florida; however, it is designed to map and track trends in large fires only (Eidenshink et al., 2007) and thus excludes most Florida fires by design. The product that underpins NEI 2014 agricultural fire emissions detected 0.9×10^5 ha of crop and pasture fires in 2014 (Pouliot et al., 2017), the only year reporting data, while the comparable number from FFS agricultural OBAs is 3.9×10^5 ha. Thus, the fire area recorded by FFS and FPA FOD is consistently about 4 times greater than detected by any of these satellite products. Even accounting for 10–20% error in the government data

(section 3), most fires and most fire area in Florida are not detected, mapped, or otherwise accounted for by current satellites.

Figure 1b shows that the discrepancies between satellite-derived fire area and FFS OBA and FPA FOD vary spatially across Florida. Both GFED and BAECV have obvious biases in northwest Florida, where prescribed silvicultural fires are widespread, but they differ from the actual fire area by a factor of 1.5–6 across most of the state (Figure S6). This detection bias is worst for small fires. Where small fires, as defined by GFED, are more 30% of the detected fire area, the mean bias is a factor of 5, but the mean bias falls to 2.7 where large fires dominate the detected fire area (Figure 1c and Text S5). The only region where GFED approaches FFS OBA and FPA FOD is on the southern shore of Lake Okeechobee, where large sugar cane fields are burned prior to harvest. BAECV, however, performs poorly in this region, due to a known weakness in detecting agricultural fires (Hawbaker et al., 2017b). Both the maps and statewide totals are consistent with fires being about four times greater than recognized from any of these satellites. Some past literature has treated Landsat-derived fire area products as more accurate than products derived from lower-resolution sensors (e.g., Boschetti et al., 2006; Giglio et al., 2009; Zhu et al., 2017), but the Florida results here caution that high-resolution sensors do not guarantee unbiased burn area estimates.

Figure 2 evaluates the temporal variability of GFED over Florida against FFS and FPA FOD data and drought indicators. Despite its overall bias, GFED reproduces the seasonal cycle of fire area, which is dominated by prescribed burning, but the multiyear GFED area anomalies (Figure 2d) closely resemble wildfire anomalies ($R^2 = 0.43$, $p < 0.001$). In fact, GFED area anomalies are uncorrelated with both total fire anomalies ($R^2 = 0.04$, $p = 0.01$) and prescribed fire anomalies in Florida ($R^2 = 0.03$, $p = 0.05$). For example, in the first half of 2010, 2014, and 2015, GFED and wildfire areas were anomalously low, but total fire area was actually well above average. These patterns are consistent with the better detection efficiency for large wildfires compared to small prescribed fires, and it means that MODIS-based sensor products may misrepresent temporal changes in fire and fire emissions in regions where humans and climate exert opposing controls on fires of various sizes. Furthermore, the satellite products can give a misleading picture of the relationship between fires and drought. GFED fire area in Florida is nearly constant or increases slightly during drought (KBDI: $R^2 = 0.1$, $p < 0.001$; PDSI: $R^2 = 0.01$, $p = 0.15$; see Text S4 for standardized precipitation index), which differs from the actual drought relationship (section 4). Thus, current satellites can misdiagnose the relationship between fire and its human and environmental drivers due to their tendency to detect large wildfires and underdetect smaller prescribed burns.

These satellite detection biases likely extend to other regions of the world with similar fire regimes to Florida. The main fire types in Florida are agriculture, savanna, and shrubland, with some temperate forest and grasslands (Figures 1 and S7); satellites underdetect fire area for all of these. Similar fire types are found throughout the world (Figure S7 and Text S5). Agricultural burning is widespread on every inhabited continent (Korontzi et al., 2006), and frequent intentional burning is used in similarly structured woodlands and savannas within parts of the U.S. Great Plains (Engle & Bidwell, 2001), South America (Cano & Leynaud, 2010; Harris et al., 2007; Mistry, 1998), sub-Saharan Africa (Coetsee et al., 2010; Savadogo et al., 2007), and Australia (Price et al., 2012; Price & Bradstock, 2010). These analogous areas account for about half of global fire emissions (Figure S7, van der Werf et al., 2017). Additionally, Florida data suggest that only 20% of fire area is detected in places where small fires, as defined by GFED, provide more than 30% of the fire area (Figure 1c). Since small fires exceed this 30% threshold in GFED data across most of the world (Figure S7), that would significantly alter detected fire area everywhere outside the boreal wildfire belt, western North America, Australia, and African savannas. Overall, the Florida data suggest that a large fraction of global fire activity and extent is currently undetected.

6. Conclusions

The combination of FFS prescribed fire data and FPA FOD wildfire data provides the most comprehensive record of fire available in Florida. Together, they report fire area of $9.9 \pm 0.7 \times 10^5$ ha/year, with uncertainty of 10%–20%. From these records, we show that multiple satellite-derived fire products underestimate burned area in Florida by approximately a factor of 4, likely due to the small size and low intensity of agricultural and silvicultural fires. Other states in the southeastern United States have similar fire regimes, so the biases documented here likely apply throughout the region and many other parts of the world with frequent prescribed burning. Correcting these biases could significantly increase the contribution of open vegetation fires to

global pollutant emissions and air quality impacts. However, updated emission estimates should also consider the accuracy of fuel load, fuel consumption, and emission factors. In particular, fuel loads tend to decrease as fires become more frequent, particularly in forests, which could partially offset changes to burn area in an emission inventory.

Emission inventories, such as NEI, could also benefit from incorporating the strong day-of-week variation seen in prescribed fire activity. The current approach of assuming uniform emissions throughout the week underestimates peak smoke emission and exposure on weekdays and overestimates them on weekends. Similar weekly patterns likely occur in other areas where prescribed fire is a common land management practice. Given that very few states and regions currently track prescribed fire, our results underscore the need for other areas to develop more comprehensive fire databases from burn authorizations and wildfire reports.

Florida fires decrease in area during drought but this is not detected by current satellite products. This relationship between fire and drought in Florida is opposite to what has been reported elsewhere, such as the Western United States, boreal zones, and the tropics (Abatzoglou & Kolden, 2013; Abatzoglou & Williams, 2016; Anderson et al., 2015; Aragão et al., 2018; Duncan et al., 2003; Randerson et al., 2012; Tosca et al., 2010; van der Werf et al., 2004, 2010; Westerling et al., 2003, 2006). Florida, likely much of the southeastern United States, and possibly other regions of the world follow a different pattern for several interlinked reasons. Prescribed fires are dominant in Florida but are restricted during drought because safety and management considerations favor burning during periods of normal rainfall. In addition, the widespread use of prescribed fires over decades likely reduces the extent and severity of wildfires, limiting their growth during drought. The Florida data therefore demonstrate that with extensive prescribed fire management, drought does not inevitably increase wildfire activity. This result shows that prescribed fire and land management can play an important role in managing drought and fire risks in the present day and under future climate change. Moreover, it suggests that prescribed fires are successfully helping to mitigate the extent and damages of wildfires during drought.

Acknowledgments
This study was supported by the NASA Atmospheric Composition Modeling and Analysis Program under grant NNX17AF60G. We thank Scott Taylor and Bryan Williams of the FFS for the OBA and KBDI data. PDSI and SPI data for Florida were obtained from NESDIS/NCDC legacy servers (https://www7.ncdc.noaa.gov/CDO/CDODivisionalSelect.jsp). GFED, BAECV, MTBS, and HMS data locations are given in the references. TTRS and DoD data are available upon request from Kevin Hiers (jkhiers@talltimbers.org).

References

Abatzoglou, J. T., & Kolden, C. A. (2013). Relationships between climate and macroscale area burned in the western United States. *International Journal of Wildland Fire*, *22*(7), 1003–1020. https://doi.org/10.1071/WF13019

Abatzoglou, J. T., & Williams, A. P. (2016). Impact of anthropogenic climate change on wildfire across western US forests. *Proceedings of the National Academy of Sciences*, *113*(42), 11,770–11,775. https://doi.org/10.1073/pnas.1607171113

Addington, R. N., Hudson, S. J., Hiers, J. K., Hurteau, M. D., Hutcherson, T. F., Matusick, G., & Parker, J. M. (2015). Relationships among wildfire, prescribed fire, and drought in a fire-prone landscape in the South-Eastern United States. *International Journal of Wildland Fire*, *24*(6), 778. https://doi.org/10.1071/WF14187

Al-Saadi, J., Soja, A. J., Pierce, R. B., Szykman, J., Wiedinmyer, C., Emmons, L. K., et al. (2008). Intercomparison of near-real-time biomass burning emissions estimates constrained by satellite fire data. *Journal of Applied Remote Sensing*, *2*(1), 021504. https://doi.org/10.1117/1.2948785

Amiro, B. D., Todd, J. B., Wotton, B. M., Logan, K. A., Flannigan, M. D., Stocks, B. J., et al. (2001). Direct carbon emissions from Canadian forest fires, 1959-1999. *Canadian Journal of Forest Research*, *31*(3), 512–525. https://doi.org/10.1139/cjfr-31-3-512

Anderson, L. O., Aragão, L. E. O. C., Gloor, M., Arai, E., Adami, M., Saatchi, S. S., et al. (2015). Global biogeochemical cycles. *Global Biogeochemical Cycles*, *29*, 1739–1753. https://doi.org/10.1002/2014GB005008.Received

Aragão, L. E. O. C., Anderson, L. O., Fonseca, M. G., Rosan, T. M., Vedovato, L. B., Wagner, F. H., et al. (2018). 21st century drought-related fires counteract the decline of Amazon deforestation carbon emissions. *Nature Communications*, *9*(1), 536–512. https://doi.org/10.1038/s41467-017-02771-y

Balch, J. K., Bradley, B. A., Abatzoglou, J. T., Nagy, R. C., Fusco, E. J., & Mahood, A. L. (2017). Human-started wildfires expand the fire niche across the United States. *Proceedings of the National Academy of Sciences*, *114*(11), 2946–2951. https://doi.org/10.1073/pnas.1617394114

Balch, J. K., Brando, P. M., Nepstad, D. C., Coe, M. T., Silvério, D., Massad, T. J., et al. (2015). The susceptibility of southeastern Amazon forests to fire: Insights from a large-scale burn experiment. *Bioscience*, *65*(9), 893–905. https://doi.org/10.1093/biosci/biv106

Bond, T. C., Doherty, S. J., Fahey, D. W., Forster, P. M., Berntsen, T. K., Deangelo, B. J., et al. (2013). Bounding the role of black carbon in the climate system: A scientific assessment. *Journal of Geophysical Research: Atmospheres*, *118*, 5380–5552. https://doi.org/10.1002/jgrd.50171

Boschetti, L., Brivio, P. A., Eva, H. D., Gallego, J., Baraldi, A., & Grégoire, J. M. (2006). A sampling method for the retrospective validation of global burned area products. *IEEE Transactions on Geoscience and Remote Sensing*, *44*(7), 1765–1773. https://doi.org/10.1109/TGRS.2006.874039

Brey, S. J., Ruminski, M., Atwood, S. A., & Fischer, E. V. (2018). Connecting smoke plumes to sources using Hazard Mapping System (HMS) smoke and fire location data over North America. *Atmospheric Chemistry and Physics*, *18*(3), 1745–1761. https://doi.org/10.5194/acp-18-1745-2018

Cano, P. D., & Leynaud, G. C. (2010). Effects of fire and cattle grazing on amphibians and lizards in northeastern Argentina (Humid Chaco). *European Journal of Wildlife Research*, *56*(3), 411–420. https://doi.org/10.1007/s10344-009-0335-7

Cardoso, M. F., Hurtt, G. C., Moore, B., Nobre, C. A., & Bain, H. (2005). Field work and statistical analyses for enhanced interpretation of satellite fire data. *Remote Sensing of Environment*, *96*(2), 212–227. https://doi.org/10.1016/j.rse.2005.02.008

Charlès, B. (2017). Spreading like wildfire. *Nature Climate Change*, *7*(11), 755–755. https://doi.org/10.1038/nclimate3432

Coetsee, C., Bond, W. J., & February, E. C. (2010). Frequent fire affects soil nitrogen and carbon in an African savanna by changing woody cover. *Oecologia*, *162*(4), 1027–1034. https://doi.org/10.1007/s00442-009-1490-y

Duncan, B. N., Martin, R. V., Staudt, A. C., Yevich, R., & Logan, J. A. (2003). Interannual and seasonal variability of biomass burning emissions constrained by satellite observations. *Journal of Geophysical Research*, *108*(D2), 4100. https://doi.org/10.1029/2002JD002378

Dwyer, E., Pinnock, S., Gregoire, J.-M., & Pereira, J. M. C. (2000). Global spatial and temporal distribution of vegetation fire as determined from satellite observations. *International Journal of Remote Sensing*, *21*(6–7), 1289–1302. https://doi.org/10.1080/014311600210182

Eidenshink, J., Schwind, B., Brewer, K., Zhu, Z., Quayle, B., & Howard, S. (2007). A project for monitoring trends in burn severity. *Fire Ecology*, *3*(1), 3–21. https://doi.org/10.4996/fireecology.0301003

Engle, D. M., & Bidwell, T. G. (2001). The response of central North American prairies to seasonal fire. *Journal of Range Management*, *54*(1), 2–10. https://doi.org/10.2458/azu_jrm_v54i1_engle

EPA. (2015a). 2011 National Emissions Inventory, version 2 Technical Support Document. Research Triangle Park, North Carolina. Retrieved from https://www.epa.gov/sites/production/files/2015-10/documents/nei2011v2_tsd_14aug2015.pdf. Accessed: 1/4/2018.

EPA. (2015b). Technical Support Document (TSD): Preparation of emissions inventories for the version 6.2, 2011 emissions modeling platform. Retrieved from http://www3.epa.gov/ttn/chief/emch/2011v6/2011v6_2_2017_2025_EmisMod_TSD_aug2015.pdf

EPA. (2016). 2014 National Emissions Inventory, version 1 Technical Support Document. Research Triangle Park, North Carolina. Retrieved from https://www.epa.gov/sites/production/files/2016-12/documents/nei2014v1_tsd.pdf

EPA. (2017). Technical Support Document (TSD): Preparation of emissions inventories for the version 7, 2014 emissions modeling platform for NATA, (June), 195. Retrieved from http://www3.epa.gov/ttn/chief/emch/2011v6/2011v6_2_2017_2025_EmisMod_TSD_aug2015.pdf

EPA. (2018). Air Emissions Modeling 2014 version 7.0 platform. Retrieved March 3, 2018, from ftp://newftp.epa.gov/air/emismod/2014/v1/ancillary_data/ge_dat_for_2014fa_nata_temporal.zip

Fernandes, P. M., & Botelho, H. S. (2003). A review of prescribed burning effectiveness in fire hazard reduction. *International Journal of Wildland Fire*, *12*(2), 117–128. https://doi.org/10.1071/WF02042

Florida Statute (2004). Florida Statute §§ 590.125(3)(b)(4) (2004).

Giglio, L., Descloitres, J., Justice, C. O., & Kaufman, Y. J. (2003). An enhanced contextual fire detection algorithm for MODIS. *Remote Sensing of Environment*, *87*(2–3), 273–282. https://doi.org/10.1016/S0034-4257(03)00184-6

Giglio, L., Loboda, T., Roy, D. P., Quayle, B., & Justice, C. O. (2009). An active-fire based burned area mapping algorithm for the MODIS sensor. *Remote Sensing of Environment*, *113*(2), 408–420. https://doi.org/10.1016/j.rse.2008.10.006

Giglio, L., Randerson, J. T., & van der Werf, G. R. (2013). Analysis of daily, monthly, and annual burned area using the fourth-generation global fire emissions database (GFED4). *Journal of Geophysical Research: Biogeosciences*, *118*, 317–328. https://doi.org/10.1002/jgrg.20042

Giglio, L., & Schroeder, W. (2007). Characterization of the tropical diurnal fire cycle using VIRS and MODIS observations. *Remote Sensing of Environment*, *108*(4), 407–421. https://doi.org/10.1016/j.rse.2006.11.018

Hall, B. L., & Brown, T. J. (2003). Comparison of precipitation and drought indices related to fire activity and potential in the US. In *Proceedings of the 5th Symposium on Fire and Forest Meteorology*. Orlando, FL: American Meteorological Society. Retrieved from Hall2003.PDF

Harris, W. N., Moretto, A. S., Distel, R. A., Boutton, T. W., & Bóo, R. M. (2007). Fire and grazing in grasslands of the argentine Caldenal: Effects on plant and soil carbon and nitrogen. *Acta Oecologica*, *32*(2), 207–214. https://doi.org/10.1016/j.actao.2007.05.001

Hawbaker, T. J., Radeloff, V. C., Syphard, A. D., Zhu, Z., & Stewart, S. I. (2008). Detection rates of the MODIS active fire product in the United States. *Remote Sensing of Environment*, *112*(5), 2656–2664. https://doi.org/10.1016/j.rse.2007.12.008

Hawbaker, T. J., Vanderhoof, M. K., Beal, Y. J., Takacs, J. D., Schmidt, G. L., Falgout, J. T., et al. (2017a). Mapping burned areas using dense time-series of Landsat data. *Remote Sensing of Environment*, *198*, 504–522. https://doi.org/10.1016/j.rse.2017.06.027

Hawbaker, T. J., Vanderhoof, M. K., Beal, Y. J., Takacs, J. D., Schmidt, G. L., Falgout, J. T., et al. (2017b). Landsat burned area essential climate variable products for the conterminous United States (1984–2015). U.S. Geological Survey data release. Retrieved from doi:https://doi.org/10.5066/F73B5X76

Heddinghaus, T. R., & Sabol, P. (1991). A review of the palmer drought severity index and where do we go from here? In *Proceedings, 7th Conf. on Applied Climatology* (pp. 242–246). Boston: American Meteorological Society.

Hu, X., Yu, C., Tian, D., Ruminski, M., Robertson, K., Waller, L. A., & Liu, Y. (2016). Comparison of the hazard mapping system (HMS) fire product to ground-based fire records in Georgia, USA. *Journal of Geophysical Research: Atmospheres*, *121*, 2901–2910. https://doi.org/10.1002/2015JD024448

Kasischke, E. S., Williams, D., & Barry, D. (2002). Analysis of the patterns of large fires in the boreal forest region of Alaska. *International Journal of Wildland Fire*, *11*(2), 131–144. https://doi.org/10.1071/WF02023

Kaulfus, A. S., Nair, U., Jaffe, D. A., Christopher, S. A., & Goodrick, S. (2017). Biomass burning smoke climatology of the United States: Implications for particulate matter air quality. *Environmental Science & Technology*, *51*(20), 11,731–11,741. https://doi.org/10.1021/acs.est.7b03292

Keetch, J. J., & Byram, G. M. (1968). A drought index for forest fire contro, USDA Forest Service Research Paper. Asheville, NC.

Korontzi, S., McCarty, J., Loboda, T., Kumar, S., & Justice, C. (2006). Global distribution of agricultural fires in croplands from 3 years of Moderate Resolution Imaging Spectroradiometer (MODIS) data. *Global Biogeochemical Cycles*, *20*, GB2021. https://doi.org/10.1029/2005GB002529

Laris, P. S. (2005). Spatiotemporal problems with detecting and mapping mosaic fire regimes with coarse-resolution satellite data in savanna environments. *Remote Sensing of Environment*, *99*(4), 412–424. https://doi.org/10.1016/j.rse.2005.09.012

Larkin, N. K., Raffuse, S. M., & Strand, T. M. (2014). Wildland fire emissions, carbon, and climate: U.S. emissions inventories. *Forest Ecology and Management*, *317*, 61–69. https://doi.org/10.1016/j.foreco.2013.09.012

Liu, Y., Goodrick, S. L., & Stanturf, J. A. (2013). Future U.S. wildfire potential trends projected using a dynamically downscaled climate change scenario. *Forest Ecology and Management*, *294*, 120–135. https://doi.org/10.1016/j.foreco.2012.06.049

Marques, S., Borges, J. G., Garcia-Gonzalo, J., Moreira, F., Carreiras, J. M. B., Oliveira, M. M., et al. (2011). Characterization of wildfires in Portugal. *European Journal of Forest Research*, *130*(5), 775–784. https://doi.org/10.1007/s10342-010-0470-4

McCarty, J. L., Korontzi, S., Justice, C. O., & Loboda, T. (2009). The spatial and temporal distribution of crop residue burning in the contiguous United States. *Science of the Total Environment*, *407*(21), 5701–5712. https://doi.org/10.1016/j.scitotenv.2009.07.009

McKee, T. B., Doesken, N. J., & Kleist, J. (1993). The relationship of drought frequency and duration to time scales. *AMS 8th Conference on Applied Climatology,* (January), 179–184. https://doi.org/citeulike-article-id:10490403

Melvin, M. A. (2015). 2015 National Prescribed Fire Use Survey Report. Retrieved from http://www.stateforesters.org/2015-national-prescribed-fire-use-survey-report

Mistry, J. (1998). Fire in the <I>cerrado</I> (savannas) of Brazil: An ecological review. *Progress in Physical Geography*, *22*(4), 425–448. https://doi.org/10.1191/030913398668494359

NIFC (2012). Fire information statistics, http://www.nifc.gov/fireInfo/fireInfo_statistics.html, Boise, Idaho.
National Oceanic and Atmospheric Administration (2017). Hazard Mapping System, January 2004 to December 2015, http://www.osdpd.noaa.gov/ml/land/hms.html, Office of Satellie and Product Operations, National Environmental Satellite, Data, And Information Service, Silver Spring, MD.
Palmer, W. C. (1965). Meteorological drought, U.S. Weather Bureau, Res. Pap. No. 45. Retrieved from https://www.ncdc.noaa.gov/temp-and-precip/drought/docs/palmer.pdf
Parisien, M.-A., Peters, V. S., Wang, Y., Little, J. M., Bosch, E. M., & Stocks, B. J. (2006). Spatial patterns of forest fires in Canada, 1980–1999. *International Journal of Wildland Fire*, *15*(3), 361. https://doi.org/10.1071/WF06009
Park, R. J., Jacob, D. J., & Logan, J. A. (2007). Fire and biofuel contributions to annual mean aerosol mass concentrations in the United States. *Atmospheric Environment*, *41*(35), 7389–7400. https://doi.org/10.1016/j.atmosenv.2007.05.061
Peterson, J. L., Lahm, P., Fitch, M., George, M., Haddow, D., Melvin, M., et al. (Eds.). (2018). NWCG smoke management guide for prescribed fire NWCG smoke management guide for prescribed fire. National Wildfire Coordination Group.
Picotte, J. J., & Robertson, K. (2011). Timing constraints on remote sensing of wildland fire burned area in the southeastern US. *Remote Sensing*, *3*(8), 1680–1690. https://doi.org/10.3390/rs3081680
Pouliot, G., Rao, V., McCarty, J. L., & Soja, A. J. (2017). Development of the crop residue and rangeland burning in the 2014 National Emissions Inventory using information from multiple sources. *Journal of the Air & Waste Management Association*, *67*(5), 613–622. https://doi.org/10.1080/10962247.2016.1268982
Prestemon, J. P., Butry, D. T., Abt, K. L., & Sutphen, R. (2010). Net benefits of wildfire prevention education efforts. *Forest Science*, *56*(2), 181–192.
Prestemon, J. P., Shankar, U., Xiu, A., Talgo, K., Yang, D., Dixon, E., et al. (2016). Projecting wildfire area burned in the south-eastern United States, 2011-60. *International Journal of Wildland Fire*, *25*(7), 715–729. https://doi.org/10.1071/WF15124
Price, O. F., & Bradstock, R. A. (2010). The effect of fuel age on the spread of fire in sclerophyll forest in the Sydney region of Australia. *International Journal of Wildland Fire*, *19*(1), 35–45. https://doi.org/10.1071/WF08167
Price, O. F., Russell-Smith, J., & Watt, F. (2012). The influence of prescribed fire on the extent of wildfire in savanna landscapes of western Arnhem Land, Australia. *International Journal of Wildland Fire*, *21*(3), 297–305. https://doi.org/10.1071/WF10079
Prichard, S. J., Stevens-Rumann, C. S., & Hessburg, P. F. (2017). Tamm review: Shifting global fire regimes: Lessons from reburns and research needs. *Forest Ecology and Management*, *396*, 217–233. https://doi.org/10.1016/j.foreco.2017.03.035
Prins, E. M., Feltz, J. M., Menzel, W. P., & Ward, D. E. (1998). An overview of GOES-8 diurnal fire and smoke results for SCAR-B and 1995 fire season in South America. *Journal of Geophysical Research*, *103*, 31,821–31,835. https://doi.org/10.1029/98JD01720
Randerson, J. T., Chen, Y., van der Werf, G. R., Rogers, B. M., & Morton, D. C. (2012). Global burned area and biomass burning emissions from small fires. *Journal of Geophysical Research*, *117*, G04012. https://doi.org/10.1029/2012JG002128
Randerson, J. T., van der Werf, G. R., Giglio, L., Collatz, G. J., & Kasibhatla, P. S. (2017). Global Fire Emissions Database, Version 4.1 (GFEDv4). Oak Ridge, TN: ORNL DAAC. Retrieved from doi:https://doi.org/10.3334/ORNLDAAC/1293
Ruminski, M., Kondragunta, S., Draxler, R., & Zeng, J. (2006). Recent changes to the hazard mapping system. In *15th International Emission Inventory Conference: Reinventing Inventories—New Ideas*. New Orleans, LA.
Savadogo, P., Sawadogo, L., & Tiveau, D. (2007). Effects of grazing intensity and prescribed fire on soil physical and hydrological properties and pasture yield in the savanna woodlands of Burkina Faso. *Agriculture, Ecosystems & Environment*, *118*(1–4), 80–92. https://doi.org/10.1016/j.agee.2006.05.002
Schichtel, B. A., Hand, J. L., Barna, M. G., Gebhart, K. A., Copeland, S., Vimont, J., & Malm, W. C. (2017). Origin of fine particulate carbon in the rural United States. *Environmental Science and Technology*, *51*(17), 9846–9855. https://doi.org/10.1021/acs.est.7b00645
Schroeder, W., Oliva, P., Giglio, L., Quayle, B., Lorenz, E., & Morelli, F. (2016). Active fire detection using Landsat-8/OLI data. *Remote Sensing of Environment*, *185*, 210–220. https://doi.org/10.1016/j.rse.2015.08.032
Schultz, M. G., Heil, A., Hoelzemann, J. J., Spessa, A., Thonicke, K., Goldammer, J. G., et al. (2008). Global wildland fire emissions from 1960 to 2000. *Global Biogeochemical Cycles*, *22*, GB2002. https://doi.org/10.1029/2007GB003031
Schweizer, D., Cisneros, R., Traina, S., Ghezzehei, T. A., & Shaw, G. (2017). Using National Ambient air Quality Standards for fine particulate matter to assess regional wildland fire smoke and air quality management. *Journal of Environmental Management*, *201*, 345–356. https://doi.org/10.1016/j.jenvman.2017.07.004
Short, K. C. (2014). A spatial database of wildfires in the United States, 1992–2011. *Earth System Science Data*, *6*(1), 1–27. https://doi.org/10.5194/essd-6-1-2014
Short, K. C. (2017). Spatial wildfire occurrence data for the United States, 1992-2015 [FPA_FOD_20170508] (4th edition). Fort Collins, CO: Forest Service Research Data Archive. doi:https://doi.org/10.2737/RDS-2013-0009.4
Soja, A. J., Al-Saadi, J., Giglio, L., Randall, D., Kittaka, C., Pouliot, G., et al. (2009). Assessing satellite-based fire data for use in the National Emissions Inventory. *Journal of Applied Remote Sensing*, *3*(1), 031504. https://doi.org/10.1117/1.3148859
Soja, A. J., Fairlie, T. D., Westberg, D. J., Pouliot, G., Ichoku, C. M., Giglio, L., & Szykman, J. J. (2011). Biomass burning plume injection height estimates using CALIOP, MODIS and the NASA langley back trajectory model. 34th International Symposium on Remote Sensing of Environment—The GEOSS Era: Towards Operational Environmental Monitoring.
Soja, A. J., Williams, D. J., Pace, T., Randall, D., & Moore, T. (2006). How well does satellite data quantify fire and enhance biomass burning emissions estimates ? 15th International Emission Inventory Conference "Reinventing Inventories - New Ideas in New Orleans, 1–18. Retrieved from http://www.epa.gov/ttnchie1/conference/ei15/
Stephens, S. L., Agee, J. K., Fule, P. Z., North, M. P., Romme, W. H., Swetnam, T. W., & Turner, M. G. (2013). Managing forests and fire in changing climates. *Science*, *342*(6154), 41–42. https://doi.org/10.1126/science.1240294
Tosca, M. G., Randerson, J. T., Zender, C. S., Flanner, M. G., & Rasch, P. J. (2010). Do biomass burning aerosols intensify drought in equatorial Asia during El Niño? *Atmospheric Chemistry and Physics*, *10*(8), 3515–3528. https://doi.org/10.5194/acp-10-3515-2010
USDA-FS & USGS (2018). Monitoring Trends in Burn Severity Fire Occurrence Dataset (2017, July - last revised). Retrieved from http://mtbs.gov/direct-download, (Accessed: 5/7/2018).
van der Werf, G. R., Randerson, J. T., Collatz, G. J., Giglio, L., Kasibhatla, P. S., Arellano, A. F., et al. (2004). Continental-scale partitioning of fire emissions during the 97/98 El Nino. *Science*, *303*(January), 73–76.
van der Werf, G. R., Randerson, J. T., Giglio, L., Collatz, G. J., Mu, M., Kasibhatla, P. S., et al. (2010). Global fire emissions and the contribution of deforestation, savanna, forest, agricultural, and peat fires (1997–2009). *Atmospheric Chemistry and Physics*, *10*(23), 11,707–11,735. https://doi.org/10.5194/acp-10-11707-2010
van der Werf, G. R., Randerson, J. T., Giglio, L., van Leeuwen, T. T., Chen, Y., Rogers, B. M., et al. (2017). Global fire emissions estimates during 1997–2016. *Earth System Science Data Discussions*, 1–43. https://doi.org/10.5194/essd-2016-62

Vicente-Serrano, S. M., Beguería, S., & López-Moreno, J. I. (2010). A multiscalar drought index sensitive to global warming: The standardized precipitation evapotranspiration index. *Journal of Climate*, *23*(7), 1696–1718. https://doi.org/10.1175/2009JCLI2909.1

Westerling, A. L., Gershunov, A., Brown, T. J., Cayan, D. R., & Dettinger, M. D. (2003). Climate and wildfire in the western United States. *Bulletin of the American Meteorological Society*, *84*(5), 595–604+548. doi:https://doi.org/10.1175/BAMS-84-5-595

Westerling, A. L., Hidalgo, H. G., Cayan, D. R., & Swetnam, T. W. (2006). Warming and earlier spring increase western U.S. Forest wildfire activity. *Science*, *313*(5789), 940–943. https://doi.org/10.1126/science.1128834

Wiedinmyer, C., Akagi, S. K., Yokelson, R. J., Emmons, L. K., Al-Saadi, J., Orlando, J. J., & Soja, A. J. (2010). The Fire INventory from NCAR (FINN)—A high resolution global model to estimate the emissions from open burning. *Geoscientific Model Development Discussion*, *3*(4), 2439–2476 . https://doi.org/10.5194/gmdd-3-2439-2010

Yokelson, R. J., Burling, I. R., Urbanski, S. P., Atlas, E. L., Adachi, K., Buseck, P. R., et al. (2011). Trace gas and particle emissions from open biomass burning in Mexico. *Atmospheric Chemistry and Physics*, *11*(14), 6787–6808. https://doi.org/10.5194/acp-11-6787-2011

Zeng, T., Wang, Y., Yoshida, Y., Tian, D., Russell, A. G., & Barnard, W. R. (2008). Impacts of prescribed fires on air quality over the southeastern United States in Spring Based on Modeling and Ground/Satellite Measurements, 8401–8406. *Environmental Science & Technology*, *42*(22), 8401–8406. https://doi.org/10.1021/es800363d

Zhu, C., Kobayashi, H., Kanaya, Y., & Saito, M. (2017). Size-dependent validation of MODIS MCD64A1 burned area over six vegetation types in boreal Eurasia: Large underestimation in croplands. *Scientific Reports*, *7*(1), 4181–4189. https://doi.org/10.1038/s41598-017-03739-0

Geophysical Research Letters

Supporting Information for

A new picture of fire extent, variability, and drought interaction in prescribed fire landscapes: insights from Florida government records

H. K. Nowell[1], C. D. Holmes[1], K. Robertson[2], C. Teske[2], and J. K. Hiers[2]

[1] Department of Earth, Ocean, and Atmospheric Science, Florida State University, Tallahassee, Florida.

[2] Tall Timbers Research Station and Land Conservancy, Tallahassee, Florida

Corresponding author: Holly Nowell (hak07@my.fsu.edu)

Contents of this file

Introduction

This supplementary information contains:

- Additional text describing our method for matching open burn authorizations (OBA) with test site fires, descriptions of fire emissions from the National Emission Inventory and the Hazard Mapping System, analysis of the standardized precipitation index (SPI), and identification of other regions in the world with similar fire regimes to Florida
- Additional figures showing test site locations, OBA to test site matching method, discussion of the current state of open fires in Florida, and global fire emissions
- Additional tables supporting the discussion of the current state of open burns in Florida and analysis of SPI

Text S1. Matching of OBA records with fires at test sites

Each fire recorded by a land manager is matched with the closest open burn authorization (OBA) on the same day. Identifying the closest OBA requires calculating the distance between each fire, identified by its centroid, and all of the OBAs on that day. To accelerate the centroid calculation, burn perimeters provided by the land manager are circumscribed by a convex hull—the polygon with minimum perimeter length that fully contains the burn area—then the centroid of the convex hull is determined. Distance calculations are carried out in ArcGIS 10.3.1 on the WGS 84 geoid using the Minimum Bounding Geometry and Feature to Point tools to construct convex hulls and locate their centroids. After pairing known fires and their OBAs, the differences in fire location and fire area are used to quantify the error in each OBA.

Matches are restricted to OBAs located on or within 1 km of the land manager's property. Some land managers, especially TTRS, request a single authorization for several nearby small burns on the same day, so we allow multiple fires to match with a single OBA. The OBA location error is the distance between the OBA point location and the centroid of its matching fire, from land manager records. When multiple fires match to a single OBA, we consider the average distance to be the error.

Figure S2 illustrates the OBA matching process on February 9, 2006 for Tyndall Air Force Base. On this day, fires were prescribed at eight different locations and two OBAs were issued in the area. Based on proximity, six burns were associated with one OBA and 2 burns with the other. For these events, the OBA location errors ranged from 2 km to 9 km. The OBAs authorized 24 ha while 1,740 ha were actually burned, giving an area error of 1716 ha (98 %). This is the largest discrepancy between requested and actual burned area in our dataset. Sect. 3 and Table S1 show that typical area errors are much smaller.

Using this approach, all but 198 of the known 4,300 fires match with OBAs. If we allow matches up to 10 km outside the site boundaries, an additional 30 burns can be matched with OBAs, but none of the OBA performance metrics (Table S1, Fig. S3) change significantly, so only the 1 km results are reported here.

Text S2. Calculating burned area from the Hazard Mapping System

HMS is derived from the following sensors and satellites: Advanced Very High Resolution Radiometer (AVHRR) on board NOAA-15/18/19 and MetOp-02/B satellites, the Geostationary Operational Environmental Satellites (GOES), and the Moderate Resolution Imaging Spectroradiometer (MODIS) on NASA's Terra and Aqua satellites (NOAA, 2017; Ruminski et al., 2006). In addition, analysts can add fires that the algorithms may have missed. Since HMS does not provide fire size information, we calculate burned area using a mean fire size derived from HMS literature. Pouliot et al. (2017) assumed that each agricultural fire in HMS was the mean size of an agricultural field for the given state (24 ha in Florida). Hu et al. (2016) matched HMS fire detections (wild and prescribed) in Georgia to ground records; they identified 36,252 fires that collectively burned 674,760 ha, which gives a mean size of 19 ha for each HMS detection. Since Florida and Georgia have similar land cover and fire practices, we assume that HMS detections in Florida also average 19 ha. According to our own analysis of FFS OBAs and FPA FOD, the median fire size in Florida is 14 ha, which includes many small fires that HMS is unlikely to detect; the mean size in Florida is 39 ha, which is heavily influenced by a few exceptionally large wildfires. Therefore, 19 ha appears to be a reasonable size to apply to HMS fire detections in Florida.

We estimate that HMS detects $2.7 \pm 0.6 \times 10^5$ ha yr^{-1} of fire in Florida, compared to $9.9 \pm 0.7 \times 10^5$ ha yr^{-1} actual fire, which is a detection efficiency of 28%. We assumed an average fire size of 19 ha per HMS detection, which is reasonable in light of past literature described above. As an upper limit, if the mean size of detected fires were twice as large, which seems unlikely given the Georgia analysis by Hu et al. (2016), HMS would still be detecting only 56% of actual fire area. Hu et

al. (2016) reported that HMS detects 60% of fire area in Georgia, much better than the 28% we find in Florida. Although land use and fire regimes in the two states are similar, several factors may explain the different results. Our results are based on 12 years of comparison while Hu et al. used only one. That particular year, 2011, had a major drought (Fig. 2c-e) in which wildfires, which are more readily detected from space, comprise a larger fraction of total fires. Hu et al. also excluded fires whose locations in the state database were recorded as a town or county (22% of fires by number) and thus under-estimated total fire activity. Finally, Georgia permitting authorities appear to deny a larger fraction of burn requests than Florida, meaning that unpermitted and unrecorded fires may be more common in Georgia. All of these factors suggest that the undetected fraction of fires in the southeastern US is probably larger than inferred by Hu et al. (2016).

Text S3. Agricultural fire emissions in the National Emission Inventory

The National Emission Inventory (NEI), constructed by the US Environmental Protection Agency (EPA), provides trace gas and aerosol emissions hourly on a 12-km grid spanning the US for air quality applications (EPA, 2017). In the NEI, non-forest agricultural crop and rangeland fires are treated similarly and separate from wildfire and prescribed forest fires. Emissions from all of these open fires are based on fire area derived from a combination of satellite detections and reporting by federal, state, and tribal agencies (EPA, 2016, 2017). NEI2014 is described here, but NEI2011 was constructed similarly.

EPA identifies agricultural fires from satellite detections filtered by land use (Pouliot et al., 2017). That method underestimates agricultural fire area in Florida, as shown in Section 5 and Table 1. States may provide their own estimates of agricultural fire emissions to EPA, in which case that overrides the satellite-detected area in the NEI (EPA, 2016). For NEI2014, the Florida Department of Environmental Protection (FDEP) submitted agricultural fire emissions as the annual total for each county in Florida (H. Walsh, FDEP, personal communication). FDEP calculated those emissions from FFS OBA fire area combined with EPA-recommended emission factors (H. Walsh; EPA, 2017). As a result, the NEI2014 estimate of agricultural fire emissions in Florida is consistent with the fire area reported here and does not suffer from the satellite detection bias documented in this work.

NEI2014 imposes a temporal profile on the annual total agricultural fire emissions provided by FDEP. The diurnal distribution assumes fires burn during daylight hours (Pouliot et al., 2017). The day-of-week distribution differs by state. For NEI2014, only Iowa specified emissions for each day of the week and, for all other states, equal burning is assumed on all days of the week (EPA, 2017). For NEI2011, nine states, not including Florida, specified the burning distribution on each day of the week (B. Henderson, US EPA, personal communication). No weekly cycle is imposed for any state in the southeastern US in either NEI2011 or NEI2014. Of the states with a weekly cycle for agriculture emissions in any NEI version, one assumes no burning on weekends (Iowa) and all others assume equal burning Monday through Friday and around 30% reduction on weekends (EPA, 2018). The weekly distribution revealed through the FFS OBAs (for agriculture and silviculture with land clearing) differs substantially from those included in the 2014 NEI (Fig. S5). Specifically, Florida fires decrease much more than 30% on weekends, but not to zero, and are not constant during the work week. Imposing a weekly cycle, as seen in Figs. 2a and S5, on agriculture and other prescribed fire in Florida would provide a clear improvement in future emission inventories. Given the similarities of agricultural and labor practices between Florida and its neighboring states, the weekly distribution identified here for Florida likely applies to other southeast US states and perhaps more broadly.

Text S4. Relationship of fire and Standardized Precipitation Index

The Standardized Precipitation Index (SPI) measures meteorological drought, which is the excess or deficit of precipitation, relative to the historical local climate normal (McKee et al., 1993). Unlike many other drought indices, including KBDI and PDSI, SPI values can be calculated over multiple time scales, to reflect short-term (1 to 6 months) and long-term (12 months and longer) drought, and compared across dissimilar regions (Hall & Brown, 2003; McKee et al., 1993; Vicente-Serrano et al., 2010). However, PDSI and KBDI have the advantage that they model soil moisture by accounting for precipitation and evaporation, thus they are more directly related to vegetation and fuel moisture. The Standardized Precipitation Evapotranspiration Index (SPEI) is similar to SPI, but additionally accounts for evapotranspiration (Vicente-Serrano et al., 2010).

We obtained SPI (from the NCDC legacy servers; calibration period from 1931-1990) and SPEI (Vicente-Serrano et al., 2010; calibration period 1950-2010; http://spei.csic.es/, accessed 6/12/2018) averages over the state of Florida (SPEI values are averages over the region cornered at 24.25°N, 79.75°W and 30.75°N, 87.75°W). SPI and SPEI time series in Florida are strongly correlated at all time scales from 3 to 24 months ($R > 0.9$, $p < 0.001$), so we report results with SPI only. SPI ranges from -3 to 3, with negative values indicating drought conditions.

Table S2 shows that wildfire area increases with drought, as measured by SPI, while prescribed fire area decreases with drought. These relationships are statistically significant ($p < 0.01$) on all SPI time scales from 3 to 24 months, but relatively weaker at the longest time scale of 24 months. Total fire area decreases during short-term drought (SPI-03) in a statistically significant way, although the relationship is weak ($R = 0.17$, $p = 0.05$). For droughts of 6 months and longer (SPI 06, 09, 12, and 24), total fire area still decreases during drought, but the relationship is not statistically significant ($p > 0.05$). We reported very similar relationships between fire and drought on different time scales in Section 4 with KBDI analogous to SPI-03 and PDSI analogous to SPI-06 or SPI-12. Indeed, Table S2 shows that KBDI is most strongly correlated to SPI-03 ($R = –0.71$) and PDSI is most strongly correlated to SPI-12 ($R = 0.87$). In Section 5, using KBDI and PDSI, we reported that GFED fire area increases slightly, if at all, during drought. As seen in Table S2, the same weak relationship is obtained with SPI as the drought indicator ($R \approx 0.2$ for SPI-03, 06, 09, and 12).

Text S5. Regions of the world with similar fire characteristics to Florida

In Section 5 and Figure S6, we showed that multiple satellite fire datasets detect only about 25% of fire area in Florida. Here we identify other regions of the world where our results may also apply based on the similarity of their fire characteristics to Florida. We identify similar fire regimes based on the prevailing fire type in GFED and whether the fires are mostly large or small, as defined by GFED. GFED version 4.1s defines fires as small if they are detected as MODIS thermal anomalies (active fires) and not detected by the MODIS burned area product (MCD64A1; van der Werf et al., 2017).

Figure S7a shows the fraction of fire area in Florida that is detected by GFED as small fires. Over most of Florida, the small fire fraction exceeds 0.5, meaning that small fires burn more area than large fires. Comparison of this small fire fraction to the map of detection biases (Fig. S6) suggests that the bias is less in areas where GFED detects mainly large fires. To quantify the effect of fire size on detection bias in a way that can be extrapolated to other regions, Figure 1c shows the ratio of reported fire area (FFS + FPA FOD) to GFED-detected fire area, as a function of the GFED small fire fraction. Each point in the figure represents a GFED grid cell in Florida with reported and detected fire areas summed over the study years 2004-2015, then divided. The mean bias ratio, weighted by fire area, is calculated for each 0.1 increment of small fire fraction and the 95% confidence intervals (CI) for the means are calculated through bootstrap resampling of the

data with replacement. Where small fires are 10% or less of the detected fire area, meaning most fires are large, the mean bias ratio is 2.7 (CI: 1.8-3.4). The mean bias increases as the small fire fraction rises, up to a bias of about 5 (CI: 3.2-7.7) where small fires account for more than 30% of the detected fire area. The 95% confidence intervals exclude a ratio of one for all values of small fire fraction, meaning that GFED under-estimates fire area in Florida regardless of which fire sizes dominate. These detection biases are almost certainly tied to fire characteristics and not the same everywhere in the globe. In particular, the biases are likely different in wildfire-dominated regions, like boreal forests and western North America, but GFED and other satellite fire products have been extensively evaluated there (Giglio et al., 2009; Randerson et al., 2012; Soja et al., 2006). Rather, the detection biases found in Florida are likely to apply in other regions of the world with prescribed agriculture fire and frequent (< 10 year return interval) intentional burning of woodlands, savannas, and shrublands.

Fire area is underestimated by satellites across all of the fire types in Florida: agriculture, savanna, and shrubland with some temperate forest (Fig. S7a). GFED data show that these fire types are not only widespread globally, but also responsible for a large portion of global fuel consumption and emissions (Fig. S7c). Agriculture fires occur on every inhabited continents (Korontzi et al., 2006) and are particularly widespread in Europe, central Asia, China, and India. In Florida, agriculture fires dominate fire activity in the region south of Lake Okeechobee. The fire area in this region, as reported by FFS, is about two times larger than what is detected by GFED. However, the detection bias for other agriculture regions of the globe could be greater because agriculture fires in this part of Florida are mostly large, as defined by GFED, while agriculture fires in most of the world are small (Fig. S7b).

Fires in the rest of Florida are a mixture of woodlands, pine savanna, shrubland, grassland, and rangeland, with some crops. In these ecosystems, fires are typically prescribed with return intervals under 10 years to mitigate wildfire risk by limiting fuel buildup and to promote biodiversity. Other regions where fires are prescribed with similar frequency in similar biomes include woodlands and savanna within the US Great Plains (Engle & Bidwell, 2001), the Cerrado, Chaco, and Caldenal of South America (Cano & Leynaud, 2010; Harris et al., 2007; Mistry, 1998), sub-Saharan African savannas (Coetsee et al., 2010; Savadogo et al., 2007), and semi-arid forests and savanna of Australia (Price et al., 2012; Price & Bradstock, 2010). Few accurate datasets of fire area have been available from these locations to test the accuracy of satellite fire products, so the similarity of their fire characteristics to Florida suggests that the satellite detection biases we have documented may apply there as well.

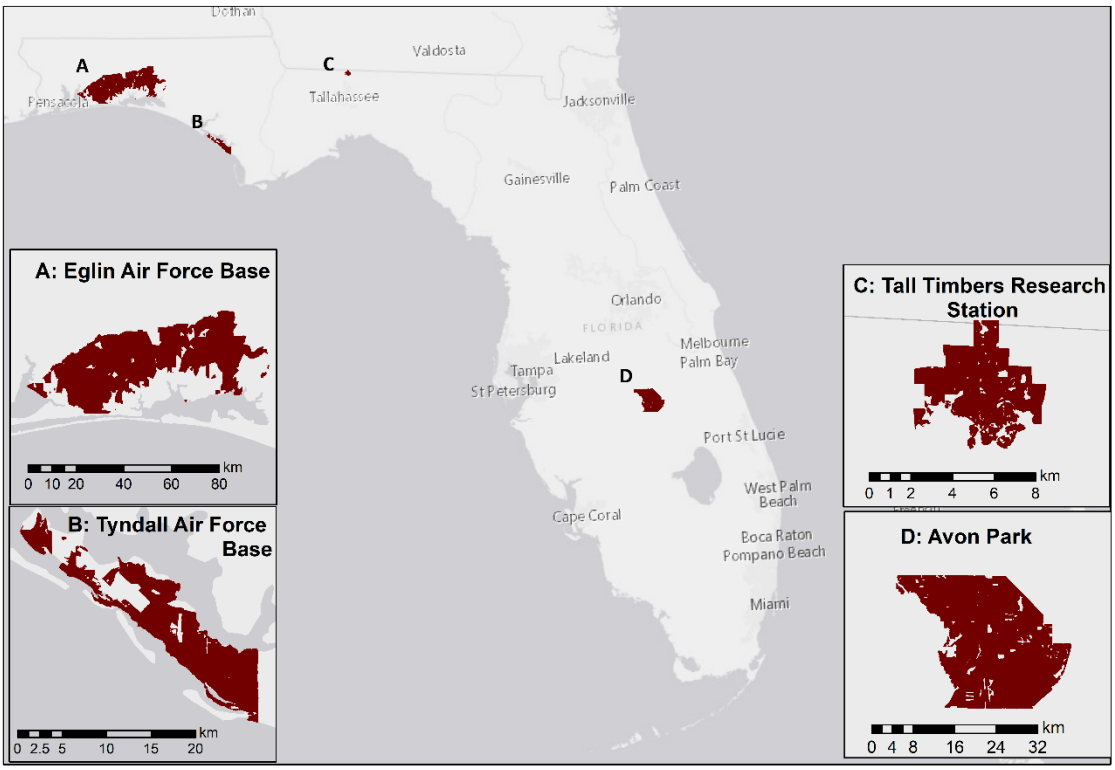

Figure S1. Evaluation sites: A) Eglin Air Force Base, B) Tyndall Air Force Base, C) Tall Timbers Research Station, and D) Avon Park Air Force Range.

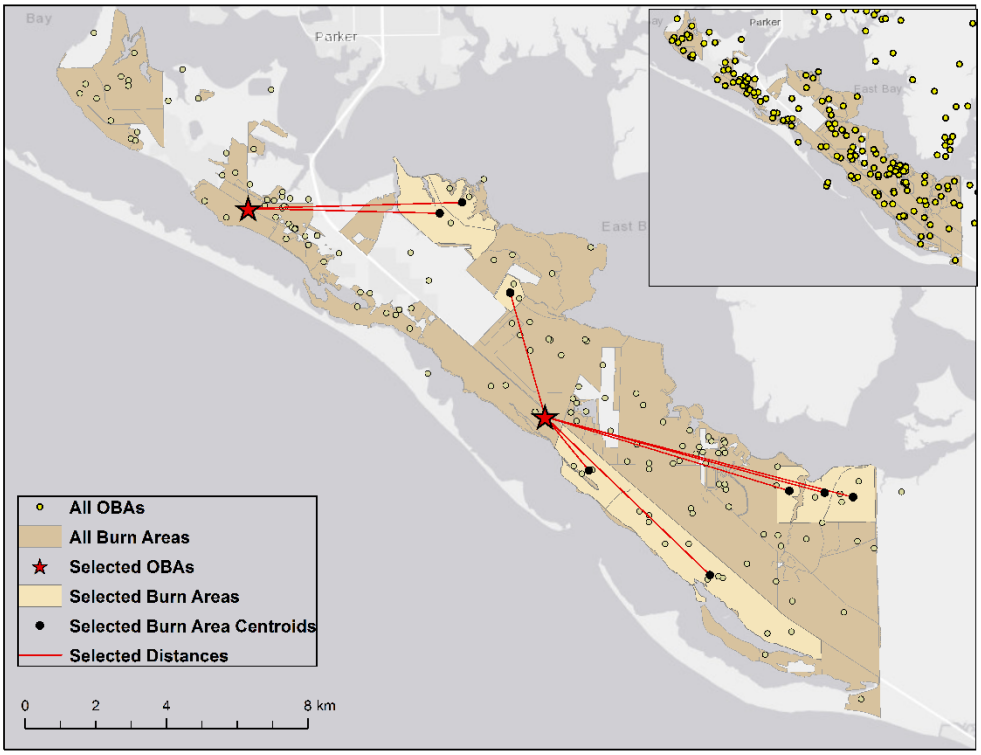

Figure S2. Example of OBA matches for prescribed fires at Tyndall Air Force Base on February 9, 2006. Yellow regions show areas burned on that day with black dots marking their centroids. Burn sites are linked (red lines) with the closest OBA issued on that date (red stars). Yellow dots show OBAs issued on other days.

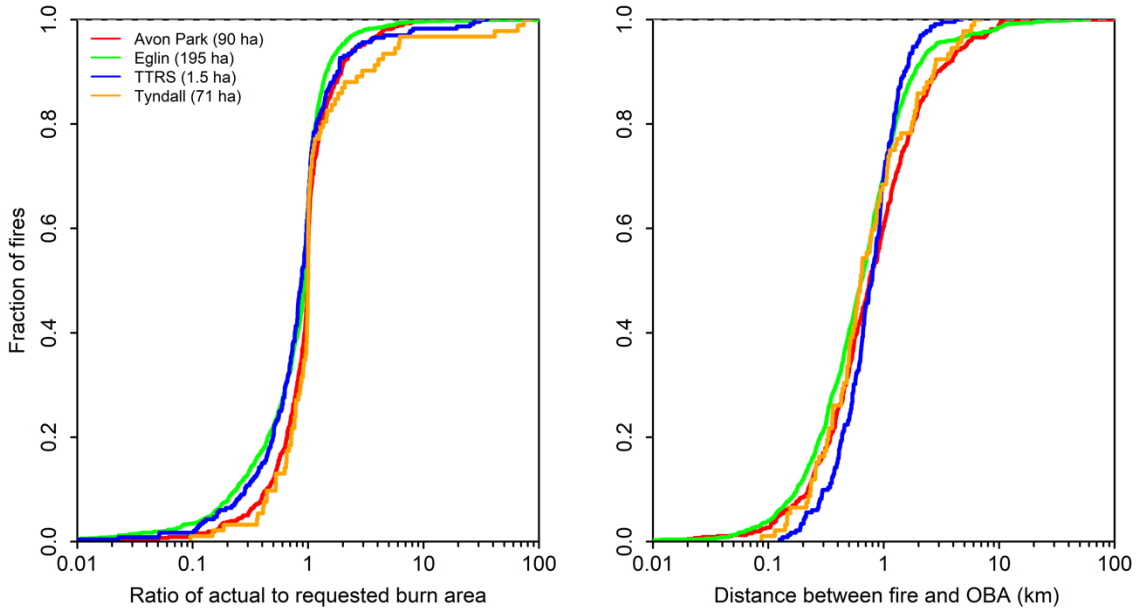

Figure S3. Cumulative distribution function (CDF) of OBA errors for fire area (left) and location (right) at four test sites for 2004-2015. When multiple burns are matched with one OBA, the average distance is used. The median burn area for each site is given in the legend in parentheses.

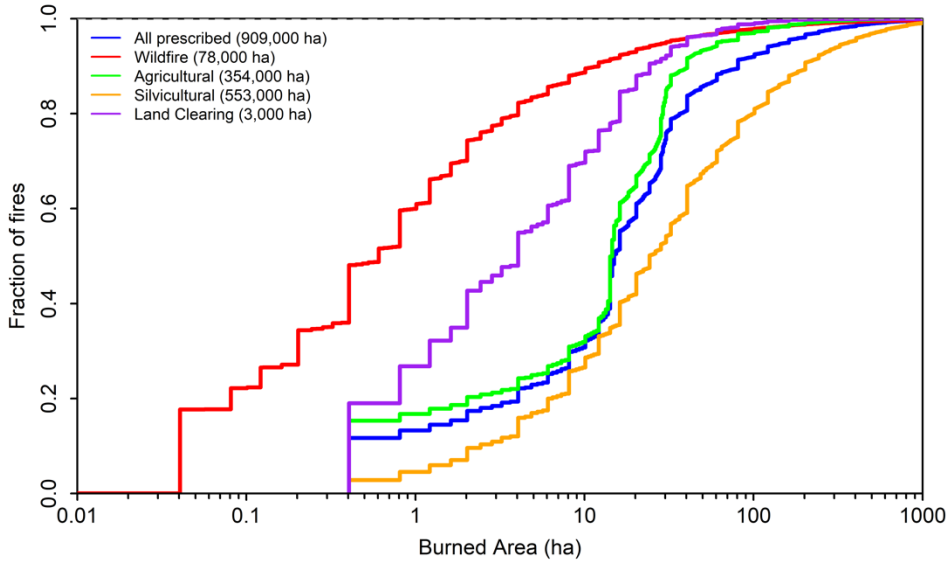

Figure S4. CDF of fire burned area for the entire state of Florida classified by type. All data are from FFS except wildfire, which is from FPA FOD (Short, 2014, 2017). The mean annual burned area associated with each type is given in the legend in parentheses.

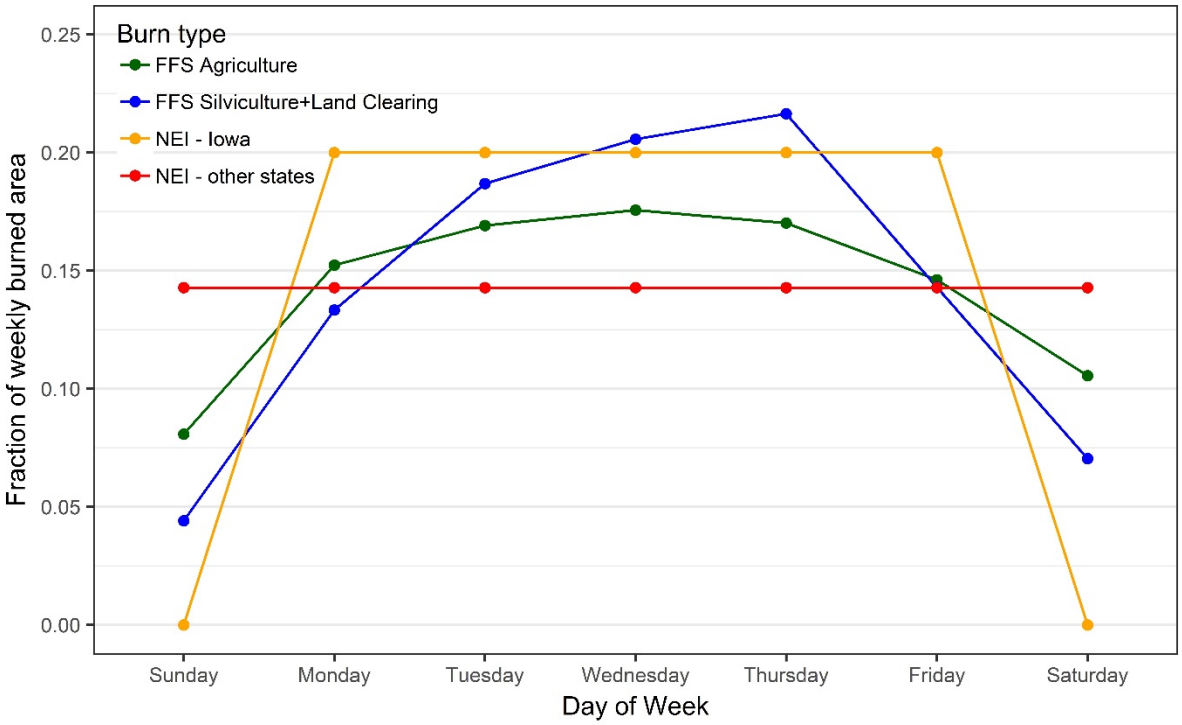

Figure S5. Distribution of burned area by day of week for FFS OBA (agriculture and silviculture plus land clearing) as compared to the 2014 NEI. In the 2014 NEI, all states were assigned a uniform distribution except for Iowa, which specified that they have no weekend prescribed fire emissions.

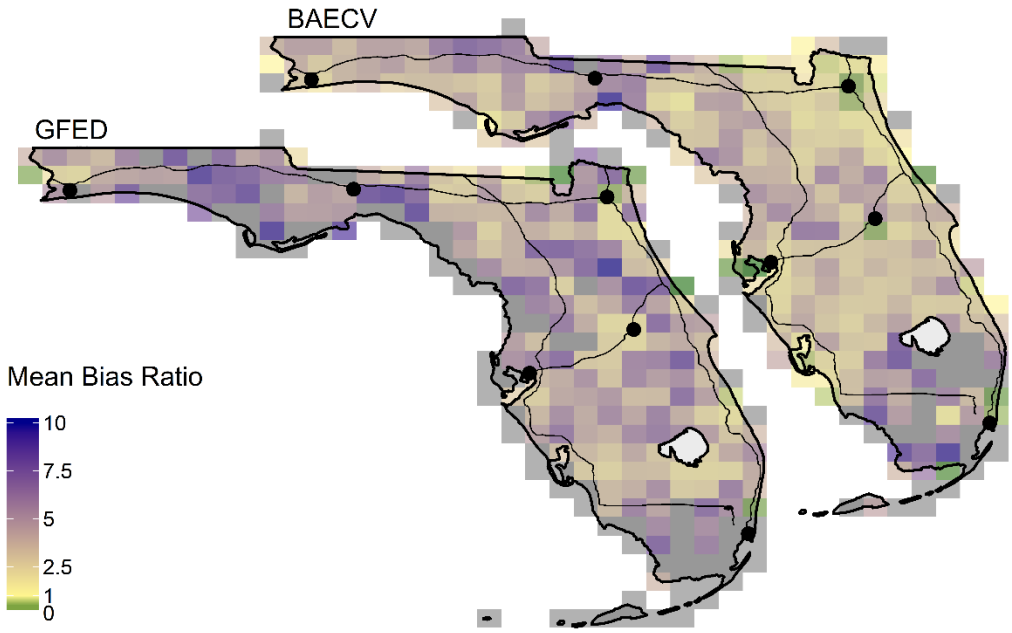

Figure S6. Mean bias of two satellite-based fire area products for 2004-2015: GFED and BAECV. Bias is shown as the mean ratio (FFS area)/(satellite-detected area) by year. Both comparisons are shown at the 0.25° GFED resolution. Note that the bias ratio values are capped at 10. For GFED, the maximum is 128 with 15% of the pixels having a bias ratio larger than 10. For BAECV, the maximum is 382 with around 5% of the pixels having a bias ratio larger than 10. Gray areas show where bias ratio is infinite because no fire was detected by the satellite product.

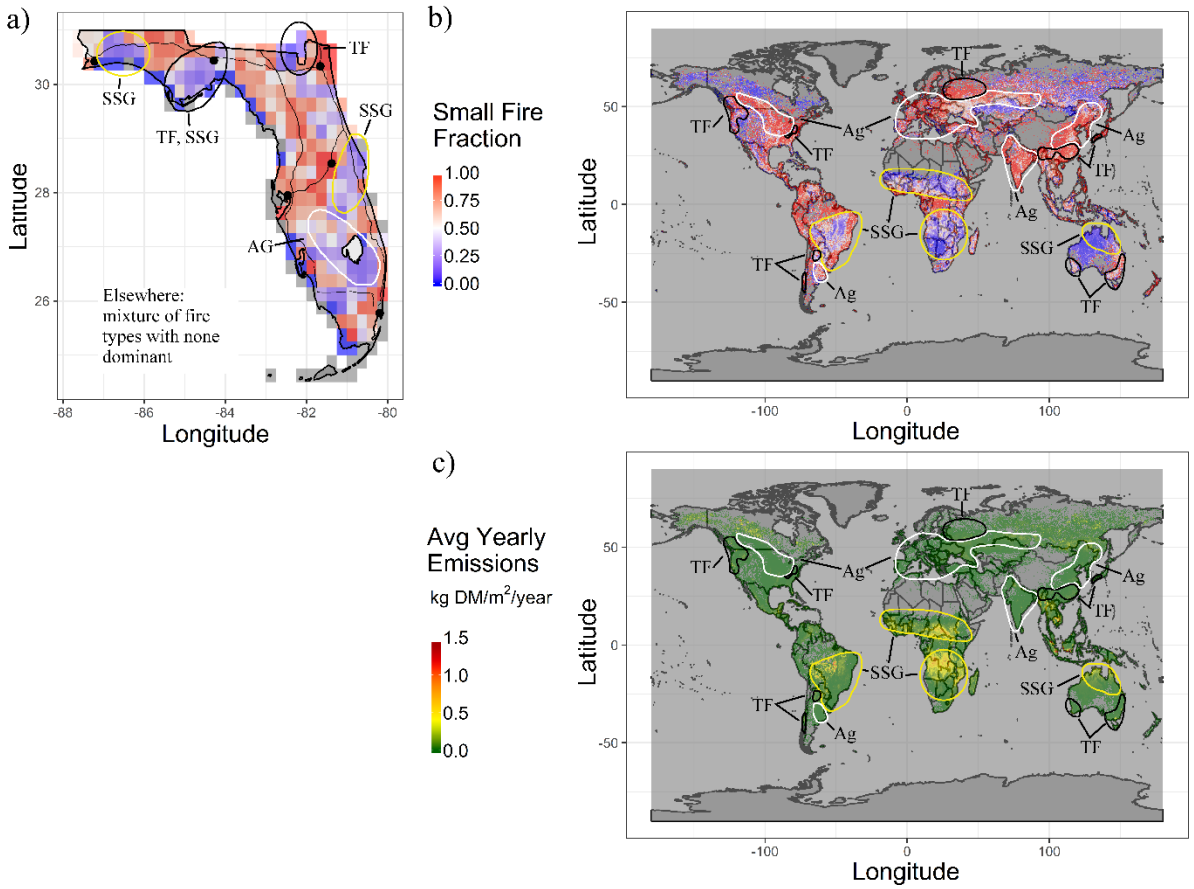

Figure S7. Fire size, type, and fuel consumption for Florida and the world, as reported by GFED: (a) the fraction of fire area detected as small fires (i.e. not detected by the MODIS burn area product) for Florida and (b) the world; (c) dry matter consumption by fire capped at 1.5 kg DM/m2/year. Outlines and text show regions where GFED classifies fuel consumption as mostly from agriculture (Ag), temperate forest (TF) or savanna, shrubland, and grassland (SSG), which are the main fire types in Florida. In Florida, TF are mainly pine savanna or flatwoods (Text S5). All results are averages over the study period of 2004-2015.

Table S1. Fire statistics and accuracy of Florida Forest Service Open Burn Authorization (OBA) database at four evaluation sites for 2004-2015.

Site[a]	Avon Park AFR	Eglin AFB	TTRS	Tyndall AFB	Total
Land area, ha	42,897	187,370	1,540	3,642	235,449
Fire area[b], ha	101,700	425,700	6,796	20,540	554,736
Number of fires[b]	681	1458	2031	130	4,300
OBA accuracy					
area error, individual fires[c,d], %	–0.9 ± 23.2	–6.5 ± 25.5	–12.7 ± 24.7	–0.4 ± 19.4	–4.3 ± 24.7
area error, cumulative[d,e], %	15.7	–13.5	–11.6	17.5	–9.2
distance error[c], km	0.77 ± 0.46	0.65 ± 0.36	0.79 ± 0.35	0.71 ± 0.39	0.74 ± 0.38
located inside perimeter, %	30	50	2	23	23

[a] Abbreviations: AFR = Air Force Range, AFB = Air Force Base, TTRS = Tall Timbers Research Station.
[b] Total for study period 2004-2015.
[c] Median error ± median absolute error.
[d] Actual fire area minus OBA area. Positive values indicate the fire area exceeded the OBA.
[e] Accumulated over entire study period 2004-2015.

Table S2. Correlation (*R*) of the standardized precipitation index (SPI) at various time scales with fire area anomalies and the PDSI and KBDI drought indices[a]

SPI period (months)	Wildfire Area Anomaly	Prescribed Fire Area Anomaly	Total Fire Area Anomaly	GFED Fire Area Anomaly	PDSI	KBDI
SPI-03	-0.48***	0.39***	0.17**	-0.21*	0.66***	-0.71***
SPI-06	-0.47***	0.33***	0.11	-0.17*	0.72***	-0.60***
SPI-09	-0.49***	0.31***	0.07	-0.22**	0.81***	-0.51***
SPI-12	-0.55***	0.41***	0.15*	-0.21*	0.87***	-0.56***
SPI-24	-0.31***	0.24***	0.09	-0.01	0.71***	-0.45***

[a] Asterisk indicates statistical significance: *** for $p < 0.01$, ** for $p < 0.05$, * for $p < 0.2$. Since SPI decreases during drought, a negative correlation coefficient (*R*) means that the quantity increases during drought. PDSI also decreases during drought, while KBDI increases during drought.